JACS
JOURNAL OF THE AMERICAN CHEMICAL SOCIETY
Article
pubs.acs.org/JACS

Microsolvation of LiI and CsI in Water: Anion Photoelectron Spectroscopy and *ab initio* Calculations

Ren-Zhong Li,[†,#] Cheng-Wen Liu,[‡] Yi Qin Gao,[*,‡] Hong Jiang,[*,‡] Hong-Guang Xu,[†] and Wei-Jun Zheng[*,†]

[†]Beijing National Laboratory for Molecular Sciences, State Key Laboratory of Molecular Reaction Dynamics, Institute of Chemistry, Chinese Academy of Sciences, Beijing 100190, China

[‡]Beijing National Laboratory for Molecular Sciences, Institute of Theoretical and Computational Chemistry, College of Chemistry and Molecular Engineering, Peking University, Beijing 100871, China

Supporting Information

ABSTRACT: In order to understand the microsolvation of LiI and CsI in water and provide information about the dependence of solvation processes on different ions, we investigated the $LiI(H_2O)_n^-$ and $CsI(H_2O)_n^-$ (n = 0–6) clusters using photoelectron spectroscopy. The structures of these clusters and their corresponding neutrals were investigated with *ab initio* calculations and confirmed by comparing with the photoelectron spectroscopy experiments. Our studies show that the structural evolutions of $LiI(H_2O)_n$ and $CsI(H_2O)_n$ clusters are very different. The Li–I distance in $LiI(H_2O)_n^-$ increases abruptly at n = 3, whereas the abrupt elongation of the Li–I distance in neutral $LiI(H_2O)_n$ occurs at n = 5. In contrast to the $LiI(H_2O)_n^-$ clusters, the Cs–I distance in $CsI(H_2O)_n^-$ increases significantly at n = 3, reaches a maximum at n = 4, and decreases again as n increases further. There is no abrupt change of the Cs–I distance in neutral $CsI(H_2O)_n$ as n increases from 0 to 6. Water molecules interact strongly with the Li ion; consequently, water molecule(s) can insert within the Li^+–I^- ion pair. In contrast, five or six water molecules are not enough to induce obvious separation of the Cs^+–I^- ion pair since the Cs–water interaction is relatively weak compared to the Li–water interaction. Our work has shown that the structural variation and microsolvation in $MI(H_2O)_n$ clusters are determined by the delicate balance between ion–ion, ion–water, and water–water interactions, which may have significant implications for the general understanding of salt effects in water solution.

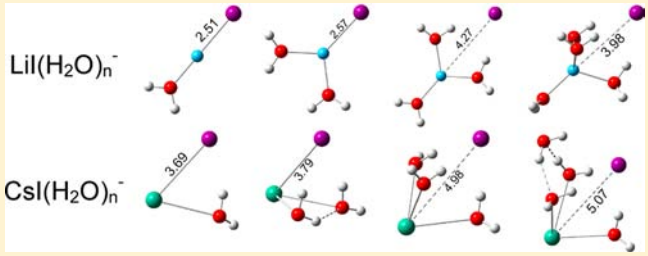

1. INTRODUCTION

Dissolution of salts is a fundamental process in chemistry. It has been suggested that salt effects on water are strongly correlated to the Hofmeister series' salting-in and salting-out effects.[1] Although solvation in the bulk solution is likely to involve a large number of water molecules and depends on the bulk properties of water, it is instructive to understand the ion–ion and ion–water interactions in small clusters. Ion–ion interactions and ion pair formation have important consequences on the dynamical properties of water,[2−4] and could also play important roles in the water/air surface tension and solvation of other molecules in water.[5,6]

Electrostatic interactions between salt ions alone lead them to exist as contact ion pairs (CIPs), in which the anion and cation interact with each other directly without interference from the solvent molecules.[7] During the solvation process, the anion and cation of the salt can be separated by the solvent molecules to form solvent-separated ion pairs (SSIPs). One interesting question is how many solvent molecules are needed to separate the CIP of a particular salt.[8] As the ionic bonds of salts can be significantly affected by the solvent molecules, it is expected that the electronic state of a SSIP would be different from that of a CIP. Thus, a reasonable approach for studying the evolution of salt CIP to SSIP structure in solvation processes is to probe the change of salt electronic state with increasing number of solvent molecules using anion photoelectron spectroscopy. Wang and co-workers have investigated $[M^+(SO_4^{2-})]_{1-2}$ (M = Na, K) ion pairs[9] and the dissolution of $NaSO_4^-$ by water[10] using anion photoelectron spectroscopy. Very recently, Feng et al. investigated the microscopic solvation of $NaBO_2$ in water by conducting photoelectron spectroscopy study and *ab initio* calculations of $NaBO_2^-(H_2O)_n$ clusters and found that the transition from the CIP structure to the SSIP structure in these clusters starts at n = 3.[11]

Alkali halides are simple salts. They play important roles in biochemistry,[12] marine chemistry,[13] and atmospheric chemistry,[14−16] as well as in our daily life. Many theoretical[8,17−35] and experimental[36−43] studies have been conducted to investigate the microscopic solvation mechanism of alkali halide salts because of their simplicity and importance. A variety of experimental techniques have been employed to study alkali halide/water clusters. Ault et al.[36] investigated alkali halide salt–water complexes using matrix-isolated infrared spectroscopy. Jouvet

Received: January 21, 2013
Published: February 23, 2013

   dx.doi.org/10.1021/ja4006942 | J. Am. Chem. Soc. 2013, 135, 5190–5199

and co-workers[37−39] studied small $NaI(H_2O)_n$ and $NaI(NH_3)_n$ clusters by resonance-enhanced two-photon ionization and femtosecond pump−probe ionization. Bowers and co-workers[41] studied the dissolution processes of Na_2I^+ and $Na_3I_2^+$ with the association of water molecules by measuring the sequential association energies of $Na_2I^+(H_2O)_n$ (n = 1−6) and $Na_3I_2^+(H_2O)_n$ (n = 1−2). Blades et al.[43] investigated the hydration energies of $(MX)_mM^+$ ions (M^+ = alkali ions or NH_4^+; X^- = halide ions, NO_2^-, or NO_3^-) using reaction-equilibration measurements. Mizoguchi et al.[42,44] studied the incipient solvation process of NaCl in water by measuring the Fourier-transform microwave spectra of $NaCl(H_2O)_n$ (n = 1−3) complexes. Regarding photoelectron spectroscopy study of these clusters, although the photoelectron spectra of a series of alkali halide anions, such as NaX^- (X = F, Cl, Br, I), KX^- (X = Cl, Br, I), and MCl^- (M = Li, Rb, Cs), were measured by Lineberger and co-workers many years ago,[45] none of the alkali halide salt−water clusters has been studied with photoelectron spectroscopy. Until now, there is no general agreement about the formation of SSIP structures for these clusters or the dependence of SSIP formation on different ions in the salts. Since photoelectron spectroscopy has been shown to be a very useful technique to explore salt−water clusters, here we investigate the $LiI(H_2O)_n^-$ and $CsI(H_2O)_n^-$ (n = 0−6) clusters using mass-selected anion photoelectron spectroscopy and *ab initio* calculations in order to understand the microsolvation of LiI and CsI in water.

The paper is organized as follows: the details of the mass-selected anion photoelectron spectroscopy experiments and *ab initio* calculations are described in section 2. The photoelectron spectra of $LiI(H_2O)_n^-$ and $CsI(H_2O)_n^-$ (n = 0−6) clusters are introduced in section 3. In section 4, the theoretical results are validated by comparison of experimental and theoretical VDEs, and the structures of the typical isomers of $LiI(H_2O)_n^-$ and $CsI(H_2O)_n^-$ (n = 0−6) clusters as well as their corresponding neutrals are examined. In section 5, the evolution of M−I distances in $MI(H_2O)_n$ clusters, the effects of different cations, and the different effects from the cations and anions are discussed.

2. EXPERIMENTAL AND COMPUTATIONAL METHODS

2.1. Experimental Methods. The experiments were conducted on a home-built apparatus consisting of a time-of-flight mass spectrometer and a magnetic-bottle photoelectron spectrometer, which has been described elsewhere.[46] Briefly, the $MI(H_2O)_n^-$ (M = Li, Cs) cluster anions were produced in a laser vaporization source by ablating a rotating, translating LiI or CsI disc target with the second harmonic (532 nm) light pulses of a Nd:YAG laser, while helium carrier gas with ∼2 atm backing pressure seeded with water vapor was allowed to expand through a pulsed valve for generating hydrated MI^- (M = Li, Cs) and cooling the formed clusters. The cluster anions were mass-analyzed by the time-of-flight mass spectrometer. The $MI(H_2O)_n^-$ (M = Li, Cs, n = 0−6) clusters were each mass-selected and decelerated before being photodetached. The electrons resulting from photodetachment were energy-analyzed by the magnetic-bottle photoelectron spectrometer. The photoelectron spectra were calibrated using the known spectrum of Pb^-.[47] The instrumental resolution was ∼40 meV for electrons with 1 eV kinetic energy.

2.2. Computational Methods. The Gaussian09[48] program package was used for all the *ab initio* calculations. The structures of $LiI(H_2O)_n^-$ and $CsI(H_2O)_n^-$ (n = 0−6) clusters and their neutral counterparts were optimized with density functional theory (DFT) employing the long-range corrected hybrid functional LC-wPBE.[49−52] We used the standard Pople-type basis 6-311++G** for Li, O, and H atoms. The effective core potential (ECP) basis sets LANL2DZdp[53] and Def2-QZVPPD,[54] as obtained from the EMSL basis set library,[55] were used for I and Cs atoms, respectively. The initial structures of the small clusters such as $LiI(H_2O)_{1-2}$ and $CsI(H_2O)_{1-2}$ were obtained by varying the positions of the water molecules. Those of the large clusters were generated from the smaller ones by adding water molecules to different positions and/or were produced by taking different snapshots from trajectories of molecular dynamics (MD) simulations. Harmonic vibrational frequencies were calculated to make sure that the optimized structures correspond to real local minima. The calculated energies were corrected by the zero-point vibrational energies. In order to confirm the reliability of the DFT calculations, the single-point energies and vertical detachment energies of the different isomers of small $LiI(H_2O)_n^-$ and $CsI(H_2O)_n^-$ clusters with n = 0−4 were also calculated with the CCSD(T) method[56] using the same basis sets. To assess the uncertainty related to the choice of different functionals, the structures of $LiI(H_2O)_n^-$ clusters were also optimized using other two variants of hybrid functionals, M06-2X[57] and wB97XD,[58] and those of $CsI(H_2O)_n^-$ (n = 0−6) clusters were optimized with the M06-2X[57] functional as well, which gave essentially the same results as LC-wPBE (see the Supporting Information).

3. EXPERIMENTAL RESULTS

The photoelectron spectra of $LiI(H_2O)_n^-$ (n = 0−6) clusters recorded with 1064 and 532 nm photons are presented in Figure 1, and those of $CsI(H_2O)_n^-$ (n = 0−6) clusters are given in

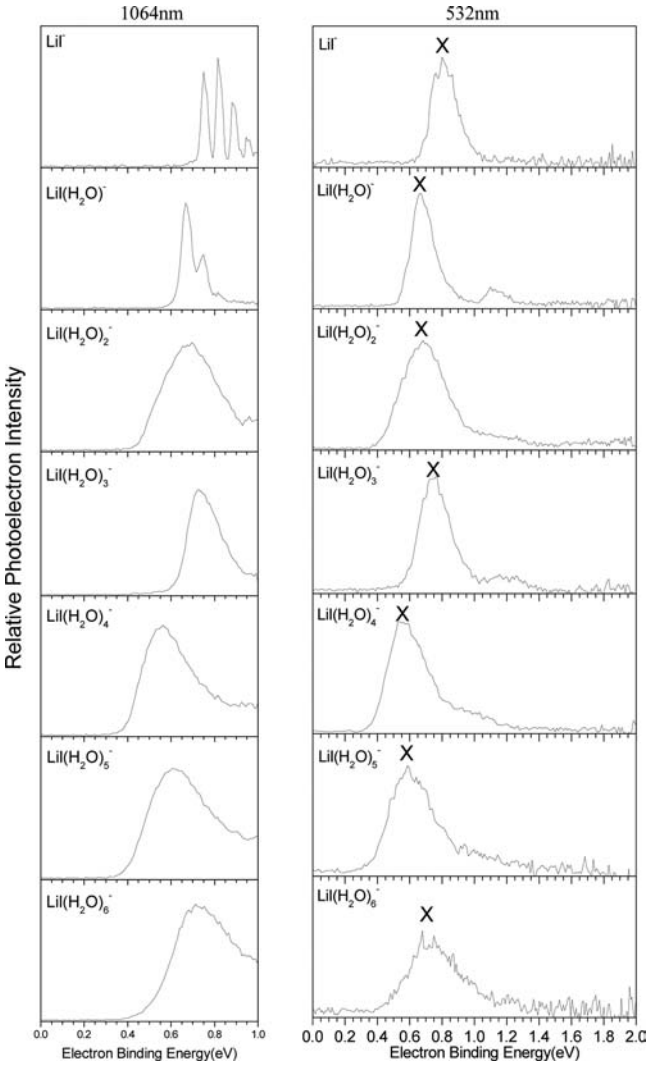

Figure 1. Photoelectron spectra of $LiI(H_2O)_n^-$ (n = 0−6) clusters recorded with 1064 and 532 nm photons.

dx.doi.org/10.1021/ja4006942 | J. Am. Chem. Soc. 2013, 135, 5190−5199

Figure 2. The vertical detachment energies (VDEs) and the adiabatic detachment energies (ADEs) of $LiI(H_2O)_n^-$ and

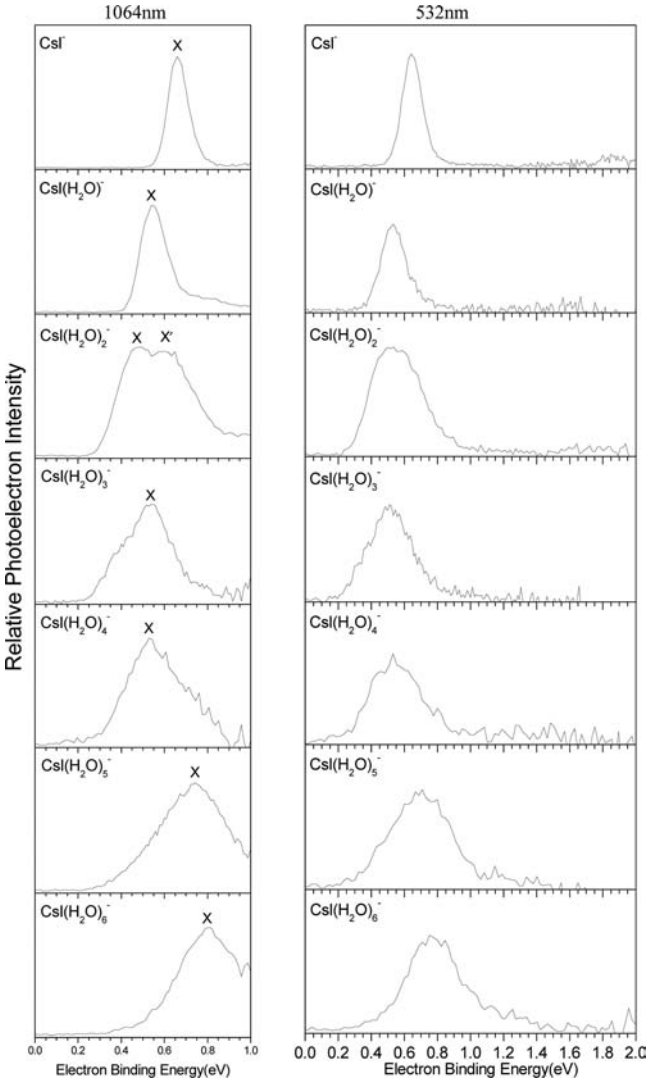

Figure 2. Photoelectron spectra of $CsI(H_2O)_n^-$ (n = 0–6) clusters recorded with 1064 and 532 nm photons.

$CsI(H_2O)_n^-$ (n = 0–6) clusters obtained from the peak positions in their photoelectron spectra are summarized in Tables 1 and 2, respectively.

The photoelectron spectrum of LiI^- recorded with 532 nm photons has an unresolved broad feature centered at 0.81 eV, which is clearly resolved into four peaks, centered at 0.754 ± 0.030, 0.820 ± 0.030, 0.889 ± 0.030, and 0.954 ± 0.030 eV in the spectrum taken with 1064 nm photons. The first peak at 0.754 eV designates the ADE, and the others correspond to the vibrational progression (Li–I stretch) of the neutral. The vibrational frequency of LiI is estimated to be 530 ± 50 cm^{-1} on the basis of the spacing of those peaks (66 meV), which is in agreement with the vibrational frequency of LiI (ω_e = 498.1 cm^{-1}) reported by Klemperer et al.[59] The VDE of LiI^- is estimated to be 0.820 ± 0.030 eV on the basis of the spectrum at 1064 nm. The peak at 0.754 eV corresponds to the transition from the vibrational ground state of LiI^- to that of LiI neutral; thus, the electron affinity of LiI is determined to be 0.754 ± 0.030 eV.

Table 1. Experimentally Observed Adiabatic Detachment Energies and Vertical Detachment Energies of $LiI(H_2O)_n^-$ (n = 0–6) from Their Photoelectron Spectra

cluster	ADE (eV)	VDE (eV)
LiI^-	0.754(±0.030)	0.820(±0.030)
$LiI(H_2O)^-$	0.670(±0.030)	0.670(±0.030)
$LiI(H_2O)_2^-$	0.48(±0.08)	0.68(±0.08)
$LiI(H_2O)_3^-$	0.64(±0.08)	0.72(±0.08)
$LiI(H_2O)_4^-$	0.41(±0.08)	0.55(±0.08)
$LiI(H_2O)_5^-$	0.42(±0.08)	0.61(±0.08)
$LiI(H_2O)_6^-$	0.50(±0.08)	0.72(±0.08)

Table 2. Experimentally Observed Adiabatic Detachment Energies and Vertical Detachment Energies of $CsI(H_2O)_n^-$ (n = 0–6) from Their Photoelectron Spectra

	X		X′
cluster	ADE (eV)	VDE (eV)	VDE (eV)
CsI^-	0.60(±0.05)	0.66(±0.05)	
$CsI(H_2O)^-$	0.46(±0.05)	0.54(±0.05)	
$CsI(H_2O)_2^-$	0.32(±0.08)	0.48(±0.08)	0.60(±0.08)
$CsI(H_2O)_3^-$	0.29(±0.15)	0.53(±0.08)	
$CsI(H_2O)_4^-$	0.33(±0.15)	0.54(±0.08)	
$CsI(H_2O)_5^-$	0.39(±0.15)	0.74(±0.08)	
$CsI(H_2O)_6^-$	0.51(±0.15)	0.80(±0.08)	

The spectrum of $LiI(H_2O)^-$ at 532 nm shows two major features, an unresolved broad feature centered at 0.67 eV and a small one centered at 1.12 eV. The feature at 1.12 eV more likely is due to the O–H stretch of the water molecule because it is higher than the first feature by ~0.45 eV (3630 cm^{-1}), close to the O–H stretch frequency of water molecules. With 1064 nm photons, the 0.67 eV broad feature can be resolved into three peaks centered at 0.670 ± 0.030, 0.745 ± 0.030, and 0.820 ± 0.030 eV. The spacing between those peaks is ~75 meV, which corresponds to a vibrational frequency of 600 ± 50 cm^{-1}. It can be assigned to the I–Li–O asymmetric stretching of $LiI(H_2O)$, as will be shown in the Theoretical Results section. The ADE and VDE of $LiI(H_2O)^-$ are both determined to be 0.670 ± 0.030 eV on the basis of the first peak in the 1064 nm spectrum.

No vibrational structure is resolved at 1064 nm for $LiI(H_2O)_n^-$ clusters with n = 2–6. The spectrum of $LiI(H_2O)_2^-$ has a very broad feature centered at 0.68 eV and a small tail between 0.9 and 1.4 eV. The spectrum of $LiI(H_2O)_3^-$ has a major peak centered at 0.72 eV and a small one centered at 1.20 eV. Similar to the case of $LiI(H_2O)^-$, the photoelectron peak of $LiI(H_2O)_3^-$ at 1.20 eV is higher than the first peak by ~0.48 eV (3871 cm^{-1}), close to the O–H stretch frequency of water molecule. The major spectral features of $LiI(H_2O)_4^-$, $LiI(H_2O)_5^-$, and $LiI(H_2O)_6^-$ are centered at 0.55, 0.61, and 0.72 eV, respectively.

Figure 2 displays the photoelectron spectra of $CsI(H_2O)_n^-$(n = 0–6) clusters, and none of them is vibrationally resolved because the vibrational frequency of CsI (ω_e = 119.2 cm^{-1})[60] is much smaller than our instrumental resolution. CsI^- has a peak centered at 0.66 eV. The VDE and ADE of CsI^- are estimated to be 0.66 ± 0.05 and 0.60 ± 0.05 eV, respectively, on the basis of the 1064 nm spectrum. Here, the ADE of CsI^- corresponds to the energy needed for the transition from the vibrational ground state of CsI^- to that of CsI neutral; therefore, the electron affinity of CsI is also 0.60 ± 0.05 eV. $CsI(H_2O)^-$ has a broad peak centered at 0.54 eV. In the spectrum of $CsI(H_2O)_2^-$ recorded with 1064 nm photons, there are two barely resolved peaks at 0.48 (X) and 0.60 eV (X′). These two peaks may come from

dx.doi.org/10.1021/ja4006942 | J. Am. Chem. Soc. 2013, 135, 5190–5199

different isomers. $CsI(H_2O)_3^-$, $CsI(H_2O)_4^-$, $CsI(H_2O)_5^-$, and $CsI(H_2O)_6^-$ all have very broad peaks, centered at 0.53, 0.54, 0.74, and 0.80 eV, respectively.

As a summary of the experimental results, Figure 3 shows the change of VDEs with the number of water molecules (n) in

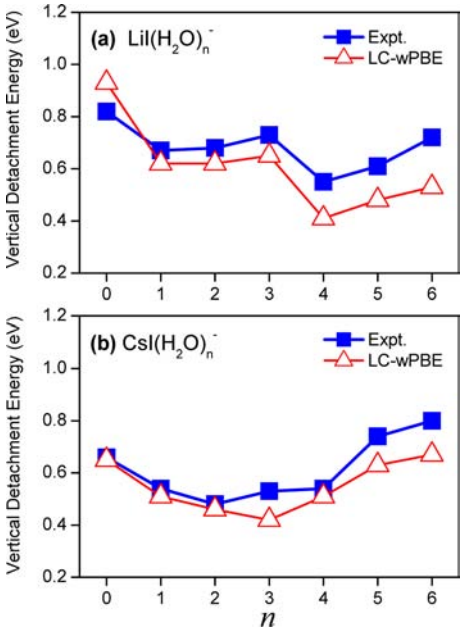

Figure 3. Experimental VDEs of $LiI(H_2O)_n^-$ and $CsI(H_2O)_n^-$ (n = 0–6) clusters compared to the VDEs of the most stable isomers of these clusters obtained with LC-wPBE method.

$LiI(H_2O)_n^-$ and $CsI(H_2O)_n^-$ (n = 0–6) clusters. We can see that the VDE of $LiI(H_2O)_n^-$ first decreases when n changes from 0 to 1, and then increases as n changes from 1 to 3, and drops again, quite dramatically, at n = 4. For $n \geq 4$, the VDE increases as the cluster size further increases. The VDE of $CsI(H_2O)_n^-$ drops constantly from n = 0 to 2, and then increases as n increases from 2 to 6. The difference between $CsI(H_2O)_3^-$ and $CsI(H_2O)_4^-$ is relatively small. As it will be discussed later, the changes of VDEs for $MI(H_2O)_n^-$ (M = Li, Cs) clusters are strongly correlated to their structural evolutions. The decrease of VDEs for $MI(H_2O)_n^-$ at $n \leq 4$ more likely implies that these water molecules interact directly with the Li and Cs atoms, while the increase of VDEs for $MI(H_2O)_n^-$ at $n \geq 4$ indicates that the fifth and sixth water molecules form hydrogen bonds with I^- or neighboring water molecules instead of interacting with the Li and Cs atoms directly. Figure 3 also shows that the VDEs of $LiI(H_2O)_n^-$ (n = 1–6) are lower than that of the bare LiI^-, and the VDEs of $CsI(H_2O)_n^-$ (n = 1–4) are lower than that of CsI^-, while those of $CsI(H_2O)_5^-$ and $CsI(H_2O)_6^-$ are higher than that of CsI^-. This difference of the VDE changes between $LiI(H_2O)_{5,6}^-$ and $CsI(H_2O)_{5,6}^-$ probably is due to the stronger interaction of the water molecules with a Li atom than with a Cs atom.

4. THEORETICAL RESULTS

We found a rather large number of low-lying isomers of $LiI(H_2O)_n^-$ and $CsI(H_2O)_n^-$ clusters, especially for n = 4–6, by theoretical calculations, consistent with the broad photoelectron spectral features of these clusters observed in the experiments, as multiple isomers may contribute to the experimental spectra. Here, we show the typical isomers of $LiI(H_2O)_n^-$ and $LiI(H_2O)_n$ (n = 0–6) in Figures 4 and 5, and those of $CsI(H_2O)_n^-$ and

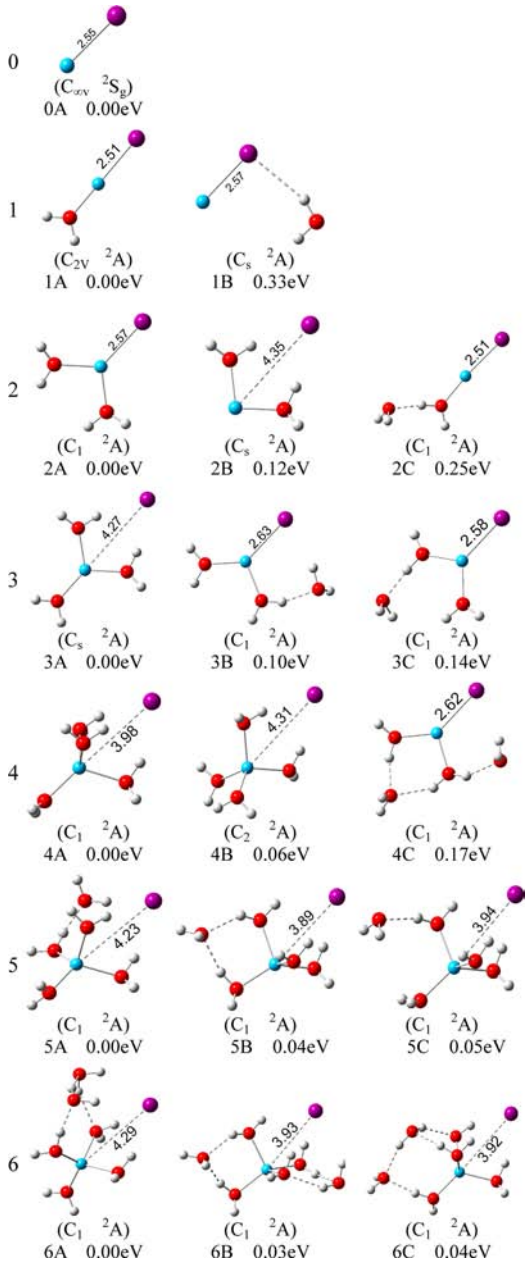

Figure 4. Optimized geometries of the typical low-lying isomers of $LiI(H_2O)_n^-$ (n = 0–6).

$CsI(H_2O)_n$ (n = 0–6) in Figures 6 and 7 (more isomers are available in the Supporting Information). The calculated relative energies, ADEs, and VDEs of these low-lying isomers are summarized and compared with the experimental values in Tables 3 and 4. The tables show that the theoretical VDEs of the most stable isomers of $LiI(H_2O)_n^-$ and $CsI(H_2O)_n^-$ are in reasonable agreement with the experimental values, indicating that these isomers, found by theoretical calculations, are likely the ones detected in the experiments. In the following paragraphs, we will examine the structures of $LiI(H_2O)_n^-$ and $CsI(H_2O)_n^-$ and their corresponding neutrals in detail in order to reveal their structural evolutions with increasing number of water molecules. It will be shown that the structures of $CsI(H_2O)_n^-$ and $CsI(H_2O)_n$ are quite different from their counterparts containing LiI.

dx.doi.org/10.1021/ja4006942 | J. Am. Chem. Soc. 2013, 135, 5190–5199

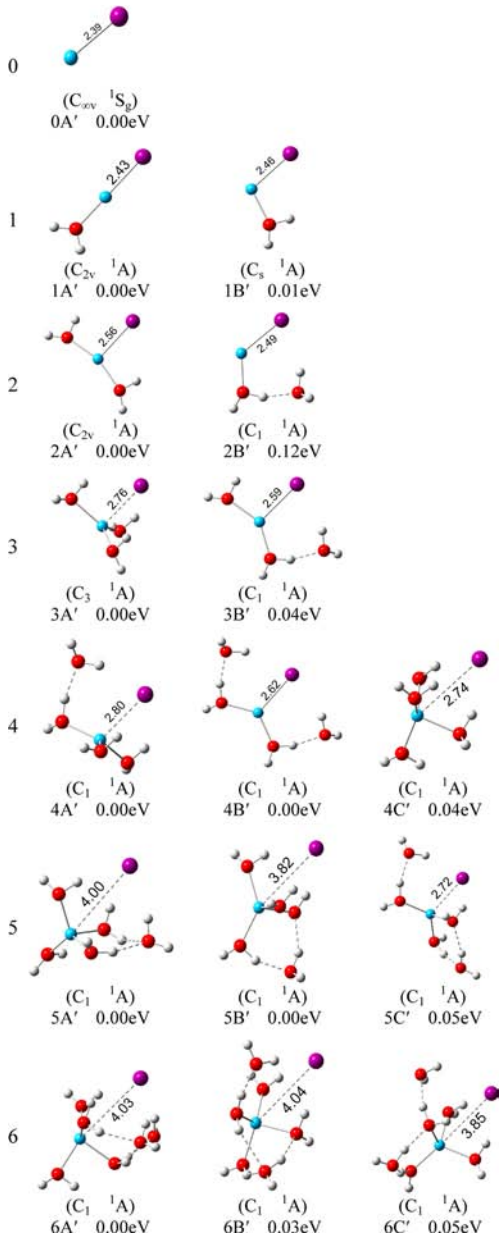

Figure 5. Optimized geometries of the typical low-lying isomers of $LiI(H_2O)_n$ (n = 0–6).

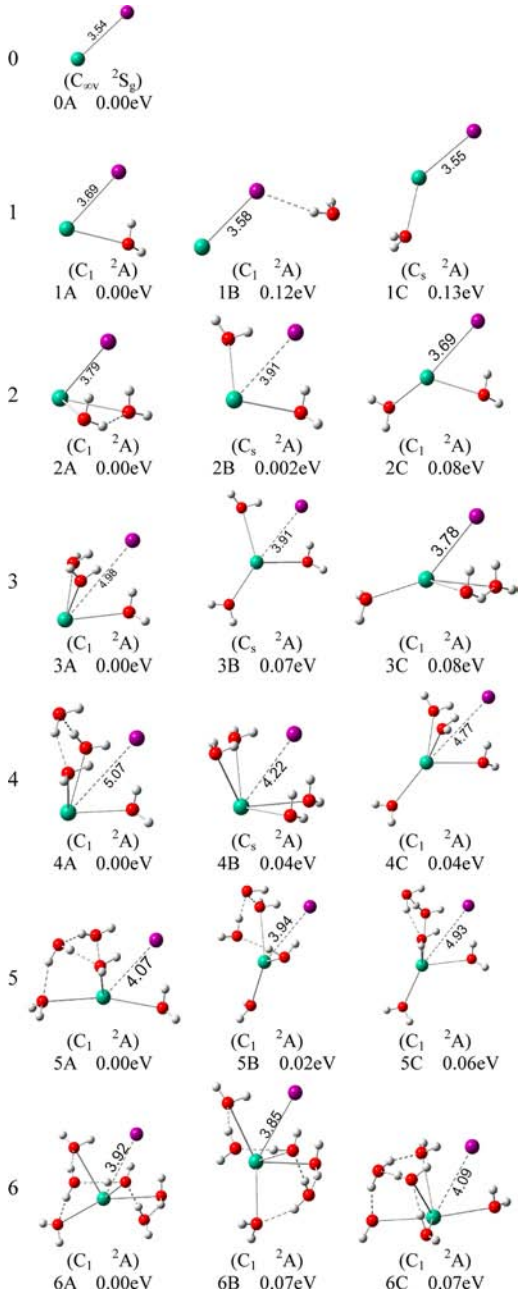

Figure 6. Optimized geometries of the typical low-lying isomers of $CsI(H_2O)_n^-$ (n = 0–6).

4.1. Structures of $LiI(H_2O)_n^-$ and $LiI(H_2O)_n$. The typical low-lying isomers of $LiI(H_2O)_n^-$ and $LiI(H_2O)_n$ (n = 0–6) are displayed in Figures 4 and 5, respectively. The results are summarized as follows.

Our calculations showed that the Li–I bond length in LiI^- is ∼2.55 Å, and in LiI neutral is ∼2.39 Å. The frequency of Li–I stretching is calculated to be ∼510 cm^{-1}, in good agreement with the experimental values of this work and Klemperer et al.[59]

The most stable structure of $LiI(H_2O)^-$ (1A) has a C_{2v} symmetry with the water molecule connected to Li atom via the O atom. Its theoretical VDE (0.62 eV) is in good agreement with the experimental value of 0.67 eV determined in Figure 1. We have also found an isomer (1B) higher in energy than isomer 1A by 0.33 eV, in which the water molecule interacts with the I atom through a hydrogen bond. But it is unlikely for isomer 1B to be produced in the experiment because it is much less stable than isomer 1A. The ground state of neutral $LiI(H_2O)$ (1A′) is similar to the most stable structure of the anion with slightly shorter Li–I distance. The I–Li–O asymmetric stretching of isomer 1A′ was calculated to be ∼622 cm^{-1} and is in agreement with the vibrational frequency of 600 ± 50 cm^{-1} observed in the photoelectron spectrum of $LiI(H_2O)^-$ taken with 1064 nm photons. The I–Li–O asymmetric stretching of $LiI(H_2O)$ was activated upon photodetachment of an electron from $LiI(H_2O)^-$ because the equilibrium bond lengths of I–Li and Li–O in $LiI(H_2O)^-$ and $LiI(H_2O)$ are different. The symmetric stretching and antisymmetric stretching of H_2O in isomer 1A′ are calculated to be 3890 and 3979 cm^{-1}, respectively, consistent with observation of the 1.12 eV peak in the experiment.

The most stable isomer of $LiI(H_2O)_2^-$ (2A) has the O atoms of the two water molecules connected to the Li atom. The Li–I distance is ∼2.57 Å. The calculated VDE of isomer 2A (0.62 eV)

dx.doi.org/10.1021/ja4006942 | J. Am. Chem. Soc. 2013, 135, 5190–5199

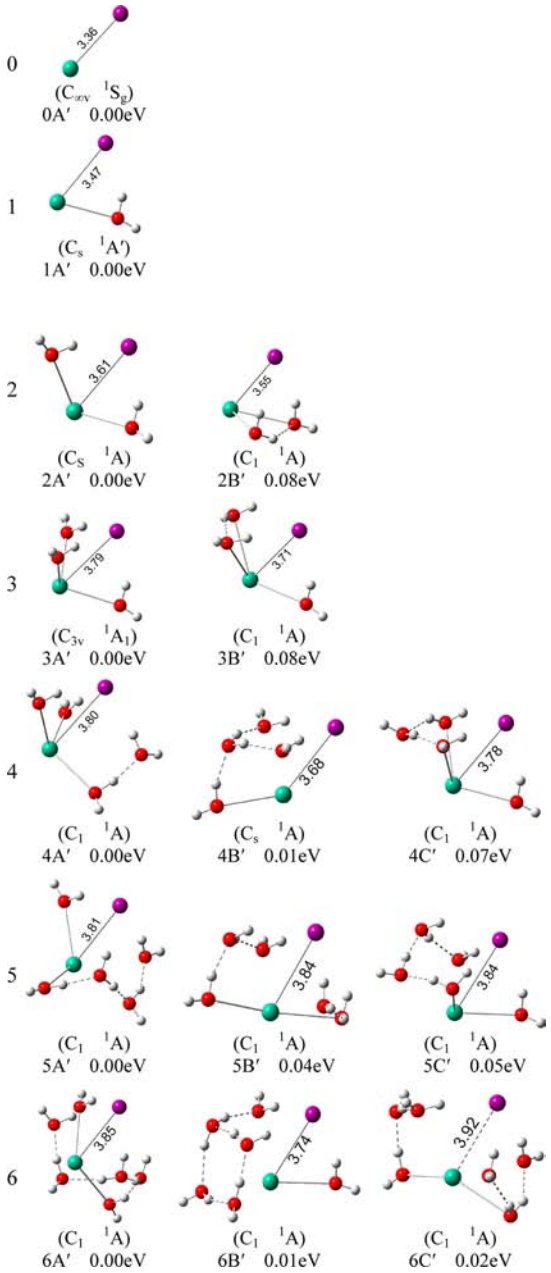

Figure 7. Optimized geometries of the typical low-lying isomers of $CsI(H_2O)_n$ (n = 0–6).

agrees well with the experimental value of 0.68 eV. The most stable isomer of neutral $LiI(H_2O)_2$ has a C_{2v} symmetry with the water molecules interacting with the Li atom via the O atom and with the I atom via H atoms. The broadening of the $LiI(H_2O)_2^-$ spectrum probably is due to the activation of the vibrational modes related to O–Li–O bending since the O–Li–O angle in neutral $LiI(H_2O)_2$ (160°) is much larger than that of $LiI(H_2O)_2^-$ (100°).

The most stable structure of $LiI(H_2O)_3^-$ has the first two water molecules between Li and I atoms, with the O atoms of water interacting with the Li atom and the H atoms of water with the I atom. The third water molecule is attached to the Li atom via its O atom. The Li–I distance in this cluster, 4.27 Å, is significantly longer than that in the smaller clusters, as a result of the insertion of two water molecules between the Li and I atoms. The position of the third water molecule in $LiI(H_2O)_3^-$ is similar to that of the water molecule in $LiI(H_2O)^-$ (1A), consistent with the observation of high electron binding energy peaks contributed by water O–H stretching in the experimental spectra of both $LiI(H_2O)^-$ (1.12 eV) and $LiI(H_2O)_3^-$ (1.20 eV). The most stable isomer of $LiI(H_2O)_3$ is a C_3 symmetric structure with three water molecules between Li and I atoms. The Li–I distance in $LiI(H_2O)_3$ neutral is ~2.76 Å, significantly shorter than that in $LiI(H_2O)_3^-$.

The most stable isomer of $LiI(H_2O)_4^-$ has three water molecules attached to both Li and I atoms, with the O atom of water interacting with the Li atom and the H atoms of water interacting with the I atom. The fourth water molecule attaches to the Li atom via its O atom and is away from the I atom. The most stable isomer of $LiI(H_2O)_4$ neutral has three water molecules interacting with the Li atom directly and the fourth water molecule interacting one of the three water molecules via a hydrogen bond.

The structures of $LiI(H_2O)_5^-$ and $LiI(H_2O)_6^-$ can be viewed as evolved from $LiI(H_2O)_4^-$ with the fifth and sixth water molecules forming hydrogen bond(s) with the other water molecules. The fifth and sixth water molecules do not interact with the Li atom directly. The structures of $LiI(H_2O)_5$ and $LiI(H_2O)_6$ neutral clusters are similar to their anionic counterparts except that the orientations of the water molecules are slightly different. In these clusters, the Li atom mainly coordinates with four water molecules, which is consistent with the commonly believed tetracoordination of Li^+ in bulk water.[61]

4.2. Structures of $CsI(H_2O)_n^-$ and $CsI(H_2O)_n$. The typical low-lying isomers of $CsI(H_2O)_n^-$ and $CsI(H_2O)_n$ (n = 0–6) are displayed in Figures 6 and 7. These structures are distinctly different from their counterparts containing LiI.

Our calculations show that the Cs–I distance in CsI^- is ~3.54 Å. The Cs–I distance in CsI neutral is ~3.36 Å, slightly shorter than that in the anion. The calculated frequency of Cs–I stretching in CsI neutral is ~116 cm^{-1}, in good agreement with the experimental value reported by Groen et al. (119.2 cm^{-1}).[60]

In the most stable structure of $CsI(H_2O)^-$, the water molecule interacts with both Cs and I atoms, with its O atom pointing to the Cs atom and one of its H atoms being directly connected to the I atom. The Cs–I distance is lengthened to 3.69 Å compared to that in bare CsI^-. The global minimum of neutral $CsI(H_2O)$ is only slightly different from that of anionic $CsI(H_2O)$.

The first two isomers of $CsI(H_2O)_2^-$, 2A and 2B, are nearly degenerate in energy, with 2B higher than 2A by only 0.002 eV. In these isomers, the two water molecules interact with both Cs and I atoms. Each of the water molecules has the O atom connected to the Cs and forms a hydrogen bond with the I atom. In isomer 2A, the two water molecules also interact with each other via a hydrogen bond, whereas in isomer 2B, the two water molecules reside on two opposite sides of the Cs–I bond without direct interaction between them. The theoretical VDEs of isomers 2A and 2B (0.46 and 0.40 eV) are consistent with the peak X observed in the 1064 nm spectrum of $CsI(H_2O)_2^-$. $CsI(H_2O)_2^-$ also has a third isomer (2C), with one water molecule interacting with both Cs and I atoms and the other water molecule connected to the Cs atom through the opposite side of the I atom. Its theoretical VDE (0.58 eV) is in agreement with the peak X′ observed in the 1064 nm spectrum of $CsI(H_2O)_2^-$. The first two isomers of $CsI(H_2O)_2$ neutral are structurally similar to those of $CsI(H_2O)_2^-$ with the order of relative stabilities switched.

In the most stable structure of $CsI(H_2O)_3^-$, the three water molecules sit between the Cs and I atoms. Each water molecule

dx.doi.org/10.1021/ja4006942 | J. Am. Chem. Soc. 2013, 135, 5190–5199

Table 3. Relative Energies of the Low-Energy Isomers of $LiI(H_2O)_n^-$ (n = 0–6) and Comparison of Their Theoretical VDEs and ADEs to the Experimental Values[a]

					VDE (eV)			ADE (eV)	
					theor			theor	
isomer		ΔE^b (eV)	symm.	state	LC-wPBE	CCSD(T)	exptl	LC-wPBE	exptl[c]
LiI^-	0A	0.00	$C_{\infty v}$	^2S_g	0.93	0.80	0.820	0.86	0.754
$LiI(H_2O)^-$	1A	0.00	C_{2v}	^2A	0.62	0.59	0.670	0.58	0.670
	1B	0.33	C_s	^2A	1.17	1.02		0.57	
$LiI(H_2O)_2^-$	2A	0.00	C_1	^2A	0.62	0.62	0.68	0.33	0.48
	2B	0.12	C_s	^2A	0.85	0.78		0.33	
	2C	0.25	C_1	^2A	0.56	0.37			
$LiI(H_2O)_3^-$	3A	0.00	C_s	^2A	0.65	0.65	0.72	0.26	0.64
	3B	0.10	C_1	^2A	0.40	0.40		0.30	
	3C	0.14	C_1	^2A	0.79	1.31		0.24	
$LiI(H_2O)_4^-$	4A	0.00	C_1	^2A	0.41	0.41	0.55	0.30	0.41
	4B	0.06	C_2	^2A	0.80	0.81		0.29	
	4C	0.17	C_1	^2A	0.57	0.58		0.29	
$LiI(H_2O)_5^-$	5A	0.00	C_1	^2A	0.48		0.61	0.23	0.42
	5B	0.04	C_1	^2A	0.65			0.24	
	5C	0.05	C_1	^2A	0.86			0.29	
$LiI(H_2O)_6^-$	6A	0.00	C_1	^2A	0.53		0.72	0.22	0.50
	6B	0.03	C_1	^2A	0.81			0.25	
	6C	0.04	C_1	^2A	0.67			0.25	

[a]The 6-311++G** basis set was used for Li, O, and H atoms. The LANL2DZdp ECP basis set was used for I atom. [b]The ΔE values are from the LC-wPBE functional. [c]Here, the experimental ADEs may not represent the real ADEs due to the possible significant structural changes between the anions and neutrals. Thus, the experimental ADEs are not used to verify the theoretical calculations.

Table 4. Relative Energies of the Low-Energy Isomers of $CsI(H_2O)_n^-$ (n = 0–6) and Comparison of Their Theoretical VDEs and ADEs to the Experimental Values[a]

					VDE (eV)			ADE (eV)	
					theor			theor	
isomer		ΔE^b (eV)	symm.	state	LC-wPBE	CCSD(T)	exptl	LC-wPBE	exptl[c]
CsI^-	0A	0.00	$C_{\infty v}$	^2S_g	0.65	0.63	0.66	0.61	0.60
$CsI(H_2O)^-$	1A	0.00	C_1	^2A	0.51	0.49	0.54	0.44	0.46
	1B	0.12	C_1	^2A	0.76	0.70		0.30	
	1C	0.13	C_s	^2A	0.72	0.75		0.27	
$CsI(H_2O)_2^-$	2A	0.00	C_1	^2A	0.46	0.44	0.48	0.39	0.32
	2B	0.00	C_s	^2A	0.40	0.38		0.31	
	2C	0.08	C_1	^2A	0.58	0.56	0.60	0.18	
$CsI(H_2O)_3^-$	3A	0.00	C_1	^2A	0.42	0.41	0.53	0.22	0.29
	3B	0.07	C_s	^2A	0.47	0.44		0.10	
	3C	0.08	C_1	^2A	0.53	0.52		0.18	
$CsI(H_2O)_4^-$	4A	0.00	C_1	^2A	0.51	0.50	0.54	0.26	0.33
	4B	0.04	C_s	^2A	0.37	0.35		0.24	
	4C	0.04	C_1	^2A	0.44	0.44		0.15	
$CsI(H_2O)_5^-$	5A	0.00	C_1	^2A	0.63		0.74	0.15	0.39
	5B	0.02	C_1	^2A	0.48			0.16	
	5C	0.06	C_1	^2A	0.56			0.05	
$CsI(H_2O)_6^-$	6A	0.00	C_1	^2A	0.67		0.80	0.26	0.51
	6B	0.07	C_1	^2A	0.71			0.22	
	6C	0.07	C_1	^2A	0.56			0.14	

[a]The 6-311++G** basis set was used for O and H atoms. The LANL2DZdp ECP basis set was used for I atom. The Def2-QZVPPD basis set was used for Cs atom. [b]The ΔE values are from the LC-wPBE functional. [c]Here, the experimental ADEs may not represent the real ADEs due to the possible significant structural changes between the anions and neutrals. Thus, the experimental ADEs are not used to verify the theoretical calculations.

has its O atom pointing to the Cs atom and one H atom pointing to the I atom; each forms a hydrogen bond with the I atom. There is no hydrogen bond between the water molecules. It is noteworthy that the Cs–I distance is lengthened significantly to

dx.doi.org/10.1021/ja4006942 | J. Am. Chem. Soc. 2013, 135, 5190–5199

4.98 Å compared to that in bare CsI^-. The global minimum structure of neutral $CsI(H_2O)_3$ is very similar to that of $CsI(H_2O)_3^-$ except that the Cs−I distance is shorter.

Many low-lying isomers of $CsI(H_2O)_4^-$, $CsI(H_2O)_5^-$, $CsI(H_2O)_6^-$, and their neutrals were found in our calculations. Basically, they all can be considered as derived from $CsI(H_2O)_3^-$. In these low-lying isomers, the fourth water molecule can interact with either the adjacent water molecules or the Cs atom. The fifth and sixth water molecules form hydrogen bonds with the other water molecules rather than interacting with the Cs atom directly. Therefore, the Cs atom is tricoordinated or tetracoordinated in these clusters.

5. DISCUSSION

5.1. Evolution of M−I Distance in $MI(H_2O)_n^{-,0}$ (M = Li, Cs) clusters. The current combined experimental and theoretical study allows us to understand how water molecules modify the interactions between cations and anions. For example, Figure 8 plots the Li−I and Cs−I distances versus the

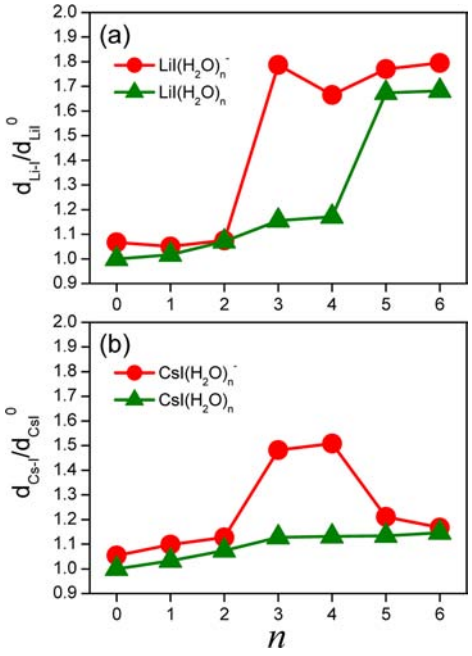

Figure 8. Evolution of M−I distances in the most stable isomers of $MI(H_2O)_n^{-,0}$ clusters (M = Li, Cs, n = 0−6). d_{LiI}^0 is the Li−I distance in LiI neutral, d_{CsI}^0 is the Cs−I distance in CsI neutral, d_{Li-I}/d_{LiI}^0 is the relative Li−I distance in $LiI(H_2O)_n^{-,0}$ clusters, and d_{Cs-I}/d_{CsI}^0 is the relative Cs−I distance in $CsI(H_2O)_n^{-,0}$ clusters.

number of water molecules in $LiI(H_2O)_n^-$ and $CsI(H_2O)_n^-$ clusters and their corresponding neutrals. Figure 8a shows that the Li−I distance in $LiI(H_2O)_n^-$ increases abruptly when n increases to 3. However, for $LiI(H_2O)_n$ neutral, such an increase of Li−I distance occurs at n = 5 instead of n = 3. The results imply that more water molecules are needed to separate the Li^+−I^- ion pair in $LiI(H_2O)_n$ neutral than in $LiI(H_2O)_n^-$ anion—five water molecules are needed to form an SSIP structure in $LiI(H_2O)_n$ neutral.

In contrast to the $LiI(H_2O)_n^-$ clusters, we can see from Figure 8b that the Cs−I distance of $CsI(H_2O)_n^-$ clusters increases slightly with cluster size during the change from n = 0 to 2, increases abruptly at n = 3, and reaches a maximum at n = 4, but, interestingly, *decreases* as n further increases. On the other hand, for $CsI(H_2O)_n$ neutral, the Cs−I distance increases very slowly with the cluster size. There is no sudden change of the Cs−I distance for $CsI(H_2O)_n$ neutral as n increases. Although the water molecules mainly stay between the Cs and I atoms, the addition of water molecules to CsI causes only slight changes in the Cs−I distance.

5.2. $MI(H_2O)_n^-$ versus $MI(H_2O)_n$ (M = Li, Cs). The M−I distances in the anionic clusters are all longer than in the corresponding neutrals. The analysis of natural bond orbital (NBO) charge distributions (see Supporting Information) showed that the metal atom is positively charged (+0.58 to +0.90 e) and the I atom is negatively charged (−0.73 to −0.90 e) in neutral $LiI(H_2O)_n$ and $CsI(H_2O)_n$ clusters, whereas the excess electron of $LiI(H_2O)_n^-$ and $CsI(H_2O)_n^-$ cluster anions mainly localizes at the metal atom side; hence, the charge is reduced to −0.18 to +0.38 e for Li and −0.09 to +0.03 e for Cs, and the negative charge of I is almost unchanged. The addition of the excess electron weakens the Coulomb attraction of the Li^+−I^- and Cs^+−I^- ion pairs. The anion−cation interactions in neutral $MI(H_2O)_n$ clusters are stronger than the metal−I^- interactions in the anionic $MI(H_2O)_n$. Thus, it is more difficult to separate the salt ion pairs in the neutral $MI(H_2O)_n$ clusters than in their anionic counterparts. This explains why the abrupt increase of Cs−I distance at n = 3 in $CsI(H_2O)_n^-$ was not observed in neutral $CsI(H_2O)_n$ and why it takes more water to separate the Li^+−I^- ion pair in neutral $LiI(H_2O)_n$ than in $LiI(H_2O)_n^-$.

5.3. $LiI(H_2O)_n^{-,0}$ versus $CsI(H_2O)_n^{-,0}$. The current study also shows that the salt−water cluster structure is strongly dependent on the ion type present. The structures of clusters containing Li are very different from their counterparts containing Cs. In the most stable structure of $LiI(H_2O)^{-,0}$ clusters, the water molecule interacts with the Li atom via its O atom from the opposite side of the I atom, while in the most stable structure of $CsI(H_2O)^{-,0}$, the water molecule sits between the Cs and I atoms with its O atom pointing to the Cs atom and one of its H atoms pointing to the I atom. In $LiI(H_2O)_2^{-,0}$ clusters, the water molecules prefer to interact with the Li atom from the opposite side of the I atom, while in $CsI(H_2O)_2^{-,0}$ clusters, the water molecules prefer to interact with both Cs and I atoms; therefore, these water molecules sit between the Cs and I atoms. Comparison of the larger $LiI(H_2O)_n^{-,0}$ and $CsI(H_2O)_n^{-,0}$ (n = 3−6) clusters also shows that the water molecules surround the Li atom more tightly than the Cs atom. The structural differences between the $CsI(H_2O)_n$ and $LiI(H_2O)_n$ clusters are due to the relatively weaker Cs^+−water interactions compared to the Li^+−water interactions, which is reasonable since the ion radius of Cs^+ is much larger than that of Li^+. The size of Li is small, and the distance between Li and I is too short for water to insert in between them without changing the Li−I interaction. The size of Cs is large, and the Cs−I distance is already very big; thus, Cs, I, and water can form a cyclic structure without changing the Cs−I distance significantly. These facts can explain why the dramatic change of the Li−I distance starts at n = 3 for $LiI(H_2O)_n^-$ anions and at n = 5 for neutral $LiI(H_2O)_n$ clusters, while the change of Cs−I distance is insignificant for $CsI(H_2O)_n^-$ and their corresponding neutrals.

Interestingly, we note that there is a significant decrease of the Cs−I distance in $CsI(H_2O)_n^-$ clusters at n = 5 and 6. This phenomenon was not observed for the $LiI(H_2O)_n^-$ clusters. In $CsI(H_2O)_n$ clusters, the Cs−water interaction is relatively weak, and the water−water interactions dominate when the number of water molecules is large. The water molecules in the second solvent shell form hydrogen bonds with the water molecules in

dx.doi.org/10.1021/ja4006942 | J. Am. Chem. Soc. 2013, 135, 5190−5199

the first shell, thus reduce the interaction between the Cs atom and the first shell water molecules. As a result, the Cs atom is close to the I atom. In contrast, in $LiI(H_2O)_n$ clusters, the water−Li interaction is more competitive than the water−water interaction. The water−water interactions do not cause significant change to the water−Li interaction; thus, the change of the Li−I distance in $LiI(H_2O)_n^-$ is much smaller at $n = 5$.

5.4. M−Water (M = Li, Cs) Interactions versus I^-−Water Interaction. Finally, from the structures of these clusters, we can see that water molecules prefer to interact with the Li or Cs atom rather than with the I atom. The water molecules stay closer to the metal atoms than to the I atom. In $LiI(H_2O)_{3-6}^{-,0}$ and $CsI(H_2O)_{5-6}^{-,0}$ clusters, the Li and Cs atoms are surrounded by water molecules while the I atom tends to stay at the surface of the clusters with only one side connecting to water molecules via hydrogen bonds. That indicates that the Li−water and Cs−water interactions are stronger than the $I^-\cdots H-O$ hydrogen bond. The exposure of I^- at the cluster surface is, interestingly, consistent with the enhanced anion concentration in iodide solutions found by MD simulations[62] and resonance-enhanced femtosecond second harmonic generation experiments.[63]

The theoretical calculations showed that the water molecules tend to interact directly with the metal atoms in small $LiI(H_2O)_n^-$ and $CsI(H_2O)_n^-$ clusters with $n \leq 4$. This observation is consistent with the evolution of VDEs measured in the experiments (Figure 3). The trends in the VDEs for $LiI(H_2O)_n^-$ and $CsI(H_2O)_n^-$ clusters are determined by the interplay of at least two major factors: (1) the addition of water molecules would increase the electron binding energy by forming hydrogen bonds with I^- or neighboring water molecules as proton donators; (2) the water molecules interacting *directly* with the Li and Cs atoms would reduce the VDEs by stabilizing the product states of photodedachment, the corresponding neutrals of $LiI(H_2O)_n^-$ and $CsI(H_2O)_n^-$, owing to the strong M^+−water interactions. In small $LiI(H_2O)_n^-$ and $CsI(H_2O)_n^-$ clusters with $n \leq 4$, the second factor dominates because the water molecules interact directly with the Li and Cs atoms; thus, the VDEs decrease in general. In the clusters with $n > 4$, the fifth and sixth water molecules do not interact directly with the Li and Cs atoms; thus, the first factor becomes more important, and the VDEs of $LiI(H_2O)_n^-$ and $CsI(H_2O)_n^-$ clusters increase significantly at $n = 5$ and 6 compared to those of $n = 4$. The experiments showed that the VDEs of $LiI(H_2O)_5^-$ and $LiI(H_2O)_6^-$ are lower than that of bare LiI^-, while those of $CsI(H_2O)_5^-$ and $CsI(H_2O)_6^-$ are higher than that of bare CsI^-, indicating that the second factor dominates more in $LiI(H_2O)_n^-$ clusters than in $CsI(H_2O)_n^-$ clusters, which is also consistent with the different structural evolutions for $LiI(H_2O)_n^-$ and $CsI(H_2O)_n^-$ clusters found by the theoretical calculations. These results demonstrate that the evolution of their photoelectron spectra with cluster size provides valuable information on the structures of the corresponding clusters.

6. CONCLUSIONS

We conducted a photoelectron spectroscopy study on mass-selected $LiI(H_2O)_n^-$ and $CsI(H_2O)_n^-$ clusters. The electron affinities of LiI and CsI were estimated to be 0.754 ± 0.030 and 0.60 ± 0.05 eV, respectively, on the basis of the photoelectron spectra of their corresponding anions. We also investigated the structures of $LiI(H_2O)_n^-$ and $CsI(H_2O)_n^-$ clusters and their corresponding neutrals by *ab initio* calculations. The most probable structures of $LiI(H_2O)_n^-$ and $CsI(H_2O)_n^-$ clusters were determined by comparison of their theoretical VDEs to the experimental values. Our studies show that the solvent-separated ion pair types of structures start to appear at $n = 3$ in $LiI(H_2O)_n^-$ cluster anions and at $n = 5$ in neutral $LiI(H_2O)_n$. However, the separation of the Cs^+-I^- ion pair by water is insignificant in $CsI(H_2O)_n$ clusters. The M−I distance in $MI(H_2O)_n^-$ (M = Li, Cs) is longer than that in $MI(H_2O)_n$, and it is easier to separate the M and I atoms in $MI(H_2O)_n^-$ than those in neutral $MI(H_2O)_n$, because the excess electron weakens the Coulomb attraction of the M^+-I^- ion pair. The effect of water−water interactions starts to show up when n increases to 5. The interactions of water molecules with Li^+ or Cs^+ are stronger than those with I^-. As a result, the I^- ion tends to stay at the cluster surface. The metal atom (cation)−I^- interaction as well as the structure of their water clusters depends strongly on the atom types. These results show the complications in the balance between different forces (cation−anion, cation−water, anion−water, and water−water interactions) which determines the structures of salt−water clusters. This study is expected to provide useful guidance in the understanding of molecular detailed interactions that determine the structures of solvated ions and ion pairs.

■ ASSOCIATED CONTENT

Supporting Information

Structures of the low-lying isomers of the $LiI(H_2O)_n^{-,0}$ and $CsI(H_2O)_n^{-,0}$ clusters; ADEs and VDEs calculated using LC-wPBE, CCSD(T), M06-2X, and wB97XD methods and their comparison with the experimental values; NBO analysis of the most stable isomers; as well as the absolute total energies and Cartesian atomic coordinates of the low-lying isomers. This material is available free of charge via the Internet at http://pubs.acs.org.

■ AUTHOR INFORMATION

Corresponding Author

gaoyq@pku.edu.cn; h.jiang@pku.edu.cn; zhengwj@iccas.ac.cn

Present Address

[#]Xi'an Polytechnic University.

Notes

The authors declare no competing financial interest.

■ ACKNOWLEDGMENTS

W.-J.Z. acknowledges the Institute of Chemistry, Chinese Academy of Sciences, for start-up funds. Y.Q.G. and H.J. thank the National Natural Science Foundation of China (21125311, 91027044, 20973009, and 21173005) for support. Part of the theoretical calculations were conducted on the ScGrid and Deepcomp7000 of the Supercomputing Center, Computer Network Information Center of Chinese Academy of Sciences. We thank the anonymous reviewers for valuable suggestions.

■ REFERENCES

(1) Tobias, D. J.; Hemminger, J. C. *Science* **2008**, *319*, 1197−1198.
(2) Buchner, R.; Capewell, S. G.; Hefter, G.; May, P. M. *J. Phys. Chem. B* **1999**, *103*, 1185−1192.
(3) Tielrooij, K. J.; Garcia-Araez, N.; Bonn, M.; Bakker, H. J. *Science* **2010**, *328*, 1006−1009.
(4) Yang, L. J.; Fan, Y. B.; Gao, Y. Q. *J. Phys. Chem. B* **2011**, *115*, 12456−12465.
(5) Gao, Y. Q. *J. Phys. Chem. B* **2011**, *115*, 12466−12472.
(6) Gao, Y. Q. *J. Phys. Chem. B* **2012**, *116*, 9934−9943.
(7) Blandame, M. J. *Chem. Rev.* **1970**, *70*, 59−93.
(8) Jungwirth, P. *J. Phys. Chem. A* **2000**, *104*, 145−148.

(9) Wang, X. B.; Ding, C. F.; Nicholas, J. B.; Dixon, D. A.; Wang, L. S. *J. Phys. Chem. A* **1999**, *103*, 3423−3429.
(10) Wang, X.-B.; Woo, H.-K.; Jagoda-Cwiklik, B.; Jungwirth, P.; Wang, L.-S. *Phys. Chem. Chem. Phys.* **2006**, *8*, 4294−4296.
(11) Feng, Y.; Cheng, M.; Kong, X.-Y.; Xu, H.-G.; Zheng, W.-J. *Phys. Chem. Chem. Phys.* **2011**, *13*, 15865−15872.
(12) Cserháti, T.; Forgács, E. *Int. J. Pharm.* **2003**, *254*, 189−196.
(13) Asmar, B. N.; Ergenzinger, P. *Hydrol. Process.* **2002**, *16*, 2819−2831.
(14) Oum, K. W.; Lakin, M. J.; DeHaan, D. O.; Brauers, T.; Finlayson-Pitts, B. J. *Science* **1998**, *279*, 74−77.
(15) Knipping, E. M.; Lakin, M. J.; Foster, K. L.; Jungwirth, P.; Tobias, D. J.; Gerber, R. B.; Dabdub, D.; Finlayson-Pitts, B. J. *Science* **2000**, *288*, 301−306.
(16) Finlayson-Pitts, B. J. *Chem. Rev.* **2003**, *103*, 4801−4822.
(17) Woon, D. E.; Dunning, T. H. *J. Am. Chem. Soc.* **1995**, *117*, 1090−1097.
(18) Peslherbe, G. H.; Ladanyi, B. M.; Hynes, J. T. *J. Phys. Chem. A* **1998**, *102*, 4100−4110.
(19) Petersen, C. P.; Gordon, M. S. *J. Phys. Chem. A* **1999**, *103*, 4162−4166.
(20) Peslherbe, G. H.; Ladanyi, B. M.; Hynes, J. T. *J. Phys. Chem. A* **2000**, *104*, 4533−4548.
(21) Yamabe, S.; Kouno, H.; Matsumura, K. *J. Phys. Chem. B* **2000**, *104*, 10242−10252.
(22) Jungwirth, P.; Tobias, D. J. *J. Phys. Chem. B* **2001**, *105*, 10468−10472.
(23) Godinho, S.; do Couto, P. C.; Cabral, B. J. C. *Chem. Phys. Lett.* **2006**, *419*, 340−345.
(24) Olleta, A. C.; Lee, H. M.; Kim, K. S. *J. Chem. Phys.* **2006**, *124*, 024321−13.
(25) Olleta, A. C.; Lee, H. M.; Kim, K. S. *J. Chem. Phys.* **2007**, *126*, 144311.
(26) Sciaini, G.; Fernandez-Prini, R.; Estrin, D. A.; Marceca, E. *J. Chem. Phys.* **2007**, *126*, 174504.
(27) Pettitt, B. M.; Rossky, P. J. *J. Chem. Phys.* **1986**, *84*, 5836−5844.
(28) Belch, A. C.; Berkowitz, M.; McCammon, J. A. *J. Am. Chem. Soc.* **1986**, *108*, 1755−1761.
(29) Smith, D. E.; Dang, L. X. *J. Chem. Phys.* **1994**, *100*, 3757−3766.
(30) Asada, T.; Nishimoto, K. *Chem. Phys. Lett.* **1995**, *232*, 518−523.
(31) Asada, T.; Nishimoto, K. *Mol. Simul.* **1996**, *16*, 307−319.
(32) Siu, C.-K.; Fox-Beyer, B. S.; Beyer, M. K.; Bondybey, V. E. *Chem.—Eur. J.* **2006**, *12*, 6382−6392.
(33) Krekeler, C.; Hess, B.; Site, L. D. *J. Chem. Phys.* **2006**, *125*, 054305.
(34) Koch, D. M.; Timerghazin, Q. K.; Peslherbe, G. H.; Ladanyi, B. M.; Hynes, J. T. *J. Phys. Chem. A* **2006**, *110*, 1438−1454.
(35) Koch, D. M.; Peslherbe, G. H. *J. Phys. Chem. B* **2008**, *112*, 636−649.
(36) Ault, B. S. *J. Am. Chem. Soc.* **1978**, *100*, 2426−2433.
(37) Gregoire, G.; Mons, M.; Dedonder-Lardeux, C.; Jouvet, C. *Eur. Phys. J. D* **1998**, *1*, 5−7.
(38) Gregoire, G.; Mons, M.; Dimicoli, I.; Dedonder-Lardeux, C.; Jouvet, C.; Martrenchard, S.; Solgadi, D. *J. Chem. Phys.* **2000**, *112*, 8794−8805.
(39) Dedonder-Lardeux, C.; Gregoire, G.; Jouvet, C.; Martrenchard, S.; Solgadi, D. *Chem. Rev.* **2000**, *100*, 4023−4037.
(40) Max, J. J.; Chapados, C. *J. Chem. Phys.* **2001**, *115*, 2664−2675.
(41) Zhang, Q.; Carpenter, C. J.; Kemper, P. R.; Bowers, M. T. *J. Am. Chem. Soc.* **2003**, *125*, 3341−3352.
(42) Mizoguchi, A.; Ohshima, Y.; Endo, Y. *J. Am. Chem. Soc.* **2003**, *125*, 1716−1717.
(43) Blades, A. T.; Peschke, M.; Verkerk, U. H.; Kebarle, P. *J. Am. Chem. Soc.* **2004**, *126*, 11995−12003.
(44) Mizoguchi, A.; Ohshima, Y.; Endo, Y. *J. Chem. Phys.* **2011**, *135*, 064307−11.
(45) Miller, T. M.; Leopold, D. G.; Murray, K. K.; Lineberger, W. C. *J. Chem. Phys.* **1986**, *85*, 2368−2375.
(46) Xu, H.-G.; Zhang, Z.-G.; Feng, Y.; Yuan, J. Y.; Zhao, Y. C.; Zheng, W. J. *Chem. Phys. Lett.* **2010**, *487*, 204−208.
(47) Feigerle, C. S.; Corderman, R. R.; Lineberger, W. C. *J. Chem. Phys.* **1981**, *74*, 1513−1515.
(48) Frisch, M. J.; et al. *Gaussian09*; Gaussian Inc: Wallingford, CT, 2009.
(49) Tawada, Y.; Tsuneda, T.; Yanagisawa, S.; Yanai, T.; Hirao, K. *J. Chem. Phys.* **2004**, *120*, 8425−8433.
(50) Vydrov, O. A.; Heyd, J.; Krukau, A. V.; Scuseria, G. E. *J. Chem. Phys.* **2006**, *125*, 074106.
(51) Vydrov, O. A.; Scuseria, G. E. *J. Chem. Phys.* **2006**, *125*, 234109.
(52) Vydrov, O. A.; Scuseria, G. E.; Perdew, J. P. *J. Chem. Phys.* **2007**, *126*, 154109.
(53) Wadt, W. R.; Hay, P. J. *J. Chem. Phys.* **1985**, *82*, 284−298.
(54) Leininger, T.; Nicklass, A.; Küchle, W.; Stoll, H.; Dolg, M.; Bergner, A. *Chem. Phys. Lett.* **1996**, *255*, 274−280.
(55) Schuchardt, K. L.; Didier, B. T.; Elsethagen, T.; Sun, L.; Gurumoorthi, V.; Chase, J.; Li, J.; Windus, T. L. *J. Chem. Inf. Model.* **2007**, *47*, 1045−1052.
(56) Pople, J. A.; Head-Gordon, M.; Raghavachari, K. *J. Chem. Phys.* **1987**, *87*, 5968−5975.
(57) Zhao, Y.; Truhlar, D. G. *J. Phys. Chem. A* **2006**, *110*, 5121−5129.
(58) Chai, J.-D.; Head-Gordon, M. *Phys. Chem. Chem. Phys.* **2008**, *10*, 6615−6620.
(59) Klemperer, W.; Norris, W. G.; Buchler, A.; Emslie, A. G. *J. Chem. Phys.* **1960**, *33*, 1534−1540.
(60) Groen, C. P.; Kovács, A. *Vibr. Spectrosc.* **2010**, *54*, 30−34.
(61) Loeffler, H. H.; Rode, B. M. *J. Chem. Phys.* **2002**, *117*, 110−117.
(62) Dang, L. X.; Chang, T.-M. *J. Phys. Chem. B* **2001**, *106*, 235−238.
(63) Petersen, P. B.; Johnson, J. C.; Knutsen, K. P.; Saykally, R. J. *Chem. Phys. Lett.* **2004**, *397*, 46−50.